AIP Journal of Applied Physics

Boron Doped diamond films as electron donors in photovoltaics: An X-ray absorption and hard X-ray photoemission study

M. Kapilashrami, G. Conti, I. Zegkinoglou, S. Nemšák, C. S. Conlon, T. Törndahl, V. Fjällström, J. Lischner, Steven G. Louie, R. J. Hamers, L. Zhang, J.-H. Guo, C. S. Fadley, and F. J. Himpsel

Citation: Journal of Applied Physics **116**, 143702 (2014); doi: 10.1063/1.4897166
View online: http://dx.doi.org/10.1063/1.4897166
View Table of Contents: http://scitation.aip.org/content/aip/journal/jap/116/14?ver=pdfcov
Published by the AIP Publishing

Articles you may be interested in

Insights on the influence of surface roughness on photovoltaic properties of state of the art copper indium gallium diselenide thin films solar cells
J. Appl. Phys. **111**, 114509 (2012); 10.1063/1.4721648

Hard x-ray photoelectron spectroscopy of chalcopyrite solar cell components
Appl. Phys. Lett. **100**, 092108 (2012); 10.1063/1.3687197

Deposition of In 2 S 3 on Cu (In , Ga) (S , Se) 2 thin film solar cell absorbers by spray ion layer gas reaction: Evidence of strong interfacial diffusion
Appl. Phys. Lett. **90**, 132118 (2007); 10.1063/1.2717534

Thin-film photovoltaics
J. Vac. Sci. Technol. A **23**, 1208 (2005); 10.1116/1.1897697

X-ray photoemission studies and energy-band diagrams of (In,Se)–CuInSe 2 /SnO 2 heterostructures
J. Appl. Phys. **82**, 825 (1997); 10.1063/1.365779

CALL FOR APPLICANTS
Seeking new Editor-in-Chief

[This article is copyrighted as indicated in the article. Reuse of AIP content is subject to the terms at: http://scitation.aip.org/termsconditions. Downloaded to] IP: 72.33.42.248 On: Wed, 08 Oct 2014 16:28:06

JOURNAL OF APPLIED PHYSICS 116, 143702 (2014)

Boron Doped diamond films as electron donors in photovoltaics: An X-ray absorption and hard X-ray photoemission study

M. Kapilashrami,[1,2] G. Conti,[3,4] I. Zegkinoglou,[1,2] S. Nemšák,[3,4] C. S. Conlon,[3,4] T. Törndahl,[5] V. Fjällström,[5] J. Lischner,[6] Steven G. Louie,[4,6] R. J. Hamers,[7] L. Zhang,[7] J.-H. Guo,[1] C. S. Fadley,[3,4] and F. J. Himpsel[2,a)]
[1]Advanced Light Source, Lawrence Berkeley National Laboratory, Berkeley, California 94720, USA
[2]Department of Physics, University of Wisconsin Madison, Madison, Wisconsin 53706, USA
[3]Department of Physics, University of California, Davis, California 95616, USA
[4]Materials Sciences Division, Lawrence Berkeley National Laboratory, Berkeley, California 94720, USA
[5]Ångström Solar Center, Uppsala University, Box 534, SE-751 21 Uppsala, Sweden
[6]Department of Physics, University of California, Berkeley, California 94720, USA
[7]Department of Chemistry, University of Wisconsin Madison, Madison, Wisconsin 53706, USA

(Received 14 July 2014; accepted 22 September 2014; published online 8 October 2014)

Highly boron-doped diamond films are investigated for their potential as transparent electron donors in solar cells. Specifically, the valence band offset between a diamond film (as electron donor) and $Cu(In,Ga)Se_2$ (CIGS) as light absorber is determined by a combination of soft X-ray absorption spectroscopy and hard X-ray photoelectron spectroscopy, which is more depth-penetrating than standard soft X-ray photoelectron spectroscopy. In addition, a theoretical analysis of the valence band is performed, based on GW quasiparticle band calculations. The valence band offset is found to be small: $VBO = VBM_{CIGS} - VBM_{diamond} = 0.3\,eV \pm 0.1\,eV$ at the CIGS/Diamond interface and $0.0\,eV \pm 0.1\,eV$ from CIGS to bulk diamond. These results provide a promising starting point for optimizing the band offset by choosing absorber materials with a slightly lower valence band maximum. © 2014 AIP Publishing LLC. [http://dx.doi.org/10.1063/1.4897166]

I. INTRODUCTION

Many solar cell materials and configurations have been developed, and these are continually being optimized.[1] Here, we start from the most general design of a solar cell, which consists of an absorber, an electron transport layer, and a hole transport layer. In the widely used Si solar cells, these three functions are combined in a single material in different doping configurations. Choosing three separate materials opens up many possibilities for new designs with enhanced performance and lower cost (see Ref. 2 for a brief overview). In the following, we will consider a generic design that takes advantage of choosing three semiconductors for the three basic functions, as shown in Fig. 1. Using transparent wide-gap semiconductors, such as TiO_2 and diamond, for the electron and hole transport layers allows both front and back illumination. At high doping, these semiconductors become metallic (and even superconducting in the case of p-doped diamond), with the Fermi level moving slightly into the band edges.

The highly doped materials for electron and hole transport can also be viewed as electron acceptors and donors, although in a context different from bulk doping. For example, the widely used n-type TiO_2 electron transport material accepts photo-excited electrons from the conduction band minimum (CBM) of the absorber, even though it contains a high density of donors in the bulk. Likewise, p-type diamond donates electrons to the absorber to fill the photo-generated holes in the absorber. These electrons do not originate from the acceptor level of diamond, but from its valence band maximum (VBM).

As absorber one needs a semiconductor with a gap near the optimum for a single junction, which lies in the 1.0–1.5 eV range. There are many semiconductors to choose from, most notably Si and GaAs. Here, we focus on CIGS (typically $Cu_y(In_{1-x}Ga_x)Se_2$), whose gap is tunable within the optimal energy range, with $x \approx 0.7$ for optimum performance.[3–11] A suitable donor has been difficult to find, particularly for dye-sensitized cells. Based on the success with TiO_2 as acceptor, we choose p-doped diamond as a symmetric counterpart. It is chemically inert, has a wide band gap making it transparent to solar radiation, and can be highly doped with boron.[12] Synthetic highly doped diamond thin films can be prepared inexpensively and are available commercially. Their structures range from microcrystalline to nanocrystalline.[13] Such films have been functionalized with dye molecules for potential applications in dye-sensitized solar cells.[14,15]

Here, we characterize the energy levels of the donor and absorber part of the proposed three-layer structure, i.e., p-type diamond and CIGS. Of particular significance for photovoltaics are the band offset and the band bending at the interface. These determine how efficiently the hole is refilled. Results from X-Ray Absorption Spectroscopy (XAS), X-ray Photoelectron Spectroscopy (XPS), and quantum efficiency measurements are combined with bulk optical and electrical properties and theoretical calculations of the quasiparticle density of states to obtain the band diagram at the interface and in the bulk. The use of multiple techniques

[a)]Author to whom correspondence should be addressed. Electronic mail: fhimpsel@wisc.edu

[This article is copyrighted as indicated in the article. Reuse of AIP content is subject to the terms at: http://scitation.aip.org/termsconditions. Downloaded to] IP: 72.33.42.248 On: Wed, 08 Oct 2014 16:28:06

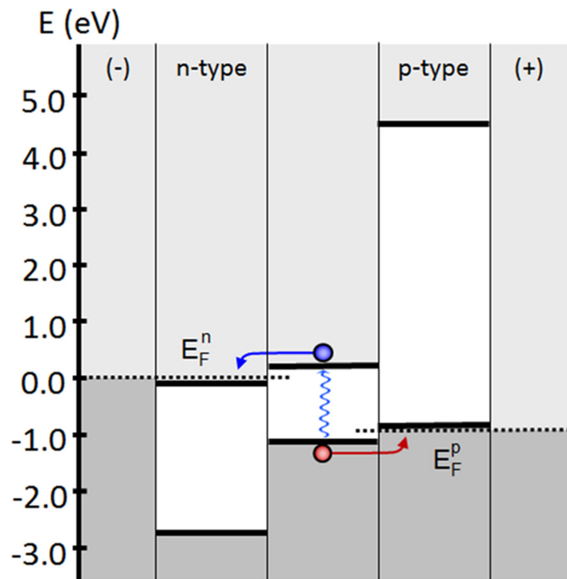

FIG. 1. Energy diagram of a generic heterojunction solar cell design using three different semiconductors, i.e., an n-doped material for electron transport (left), a photon absorber (center), and a p-doped material for hole transport (right). Small band offsets at the interfaces maximize the open circuit photovoltage, which is given by the difference between the Fermi levels in the p- and n-doped semiconductors.

provides redundancy and allows for cross-checks of the accuracy. We find the VBM of CIGS to be 0.3 ± 0.1 eV higher than the VBM of p-doped diamond at the interface, and 0.0 ± 0.1 eV higher than the bulk VBM of diamond. These represent small barriers for hole transport. To eliminate them completely, it is proposed to substitute Se by S in CIGS or to choose an absorber material with a somewhat lower VBM. The width of the interface barrier can be reduced by higher B doping.

The paper is organized as follows: After a discussion of the experimental details in Sec. II, we proceed to the determination of the unoccupied states by XAS in Sec. III and to measurements of occupied states by XPS in Sec. IV. Since the valence band offset is between occupied states, it can be determined by XPS alone, as done in Table I. But the inclusion of more accurate literature data for bulk diamond allows a refinement of the results, particularly for the VBM relative to the Fermi level and to the C1*s* core level. This refinement is performed in Sec. V, and the complete band diagram is given in Fig. 5. It combines the most accurate available results and includes both occupied and unoccupied states. The key findings and their consequences for using diamond as electron donor material are presented in Sec. VI.

II. EXPERIMENTS

A 7 nm thin film of $Cu_{0.78}(In_{0.32}Ga_{0.68})Se_2$ with Cu/[Ga + In] = 78% and Ga/[Ga + In] = 68% was deposited by co-evaporation of Cu, In, Ga, and Se at a substrate temperature of 540 °C, in a base-pressure $<3 \times 10^{-6}$ mbar) on a polycrystalline diamond substrate at. The composition was obtained from a 2.3 μm thick reference sample by X-ray fluorescence, using an XRF Panalytical Epsilon 5. The polished surface of a p-doped polycrystalline diamond substrate (boron concentration about $10^{20}\,cm^{-3}$) from Element Six Ltd. (Ascot. Berkshire, SL5 8BP, UK) was H-passivated in a 50 Torr hydrogen plasma, as described previously.[16] In addition to the 7 nm CIGS/Diamond heterojunction sample, two reference samples were analyzed, a 2.3 μm thick CIGS ($Cu_{0.78}(In_{0.32}Ga_{0.68})Se_2$) film deposited on a Mo coated soda-lime glass substrate and a H-terminated, p-doped polycrystalline diamond substrate.

The 2.3 μm CIGS film on Mo-coated soda-lime glass was processed into a complete PV device, shown in Fig. 2(a), following the Ångström baseline procedure (as described in Ref. 17). The I-V characteristics of this device were measured at a cell temperature of 25 °C and under light illumination from an ELH light source (1000 W/m^2). Representative values for all 32 cells on the 5 × 5 cm CIGS/Mo sample are an open circuit voltage of 0.8 V, a short circuit current of 22.3 mA/cm^2, a fill factor of 78.5%, and a conversion efficiency of 13.7%.

The external quantum efficiency was determined from 300 nm to 1050 nm in 2 nm intervals, using chopped monochromatic light from a Xe-arc light source (calibrated by Si and InGaAs photodiodes). The optical band gap (E_g) of our CIGS film was estimated by linear extrapolation of the absorption edge of the quantum efficiency spectra (Fig. 2(b)). The resulting value $E_g = 1.4$ eV is consistent with the relation between E_g and x obtained in Ref. 18 using x = Ga/[Ga + In] = 0.68:

$$E_g = 1.01 + 0.626 \cdot x - 0.167 \cdot (1 - x). \tag{1}$$

For our analysis, we have assumed that E_g of the 7 nm CIGS layer on diamond is the same as for the 2.3 μm thick film used to acquire the optical data. Possible differences in E_g could be caused by different growth modes or different stoichiometry. Grazing incidence X-ray diffraction data for the thin sample were shifted 0.1–0.2° towards lower diffracting angles, indicating that the 7 nm sample is slightly more In-rich than the 2.3 μm sample, resulting in $x \approx 0.5$. That would reduce the band gap by ≈ 0.1 eV for the 7 nm sample, which

TABLE I. Core level positions and VBM (reference samples and interface) obtained from high energy HXPS (hv = 5.0 kV) relative to the Fermi level $E_F = 0$. The VBM of the CIGS reference sample is determined by linear extrapolation and the VBM of diamond by matching the spectrum to the self-consistent GW calculation. The valence band offset (VBO) is obtained using Eq. (2), and the VBM positions in diamond and CIGS at the interface using Eq. (3).

Sample	C1*s*	Cu2$p_{3/2}$	VBM from Fig. 4	VBM from Eq. (3)	VBO from Eq. (2)
H-terminated diamond (reference)	284.19 eV		0.45 eV		
Bulk CIGS(reference)		932.3 eV	0.31 eV		
CIGS/Diamond	284.24 eV	932.22 eV		$VBM_{Diamond} = 0.5$ eV $VBM_{CIGS} = 0.23$ eV	0.27 eV

[This article is copyrighted as indicated in the article. Reuse of AIP content is subject to the terms at: http://scitation.aip.org/termsconditions. Downloaded to] IP: 72.33.42.248 On: Wed, 08 Oct 2014 16:28:06

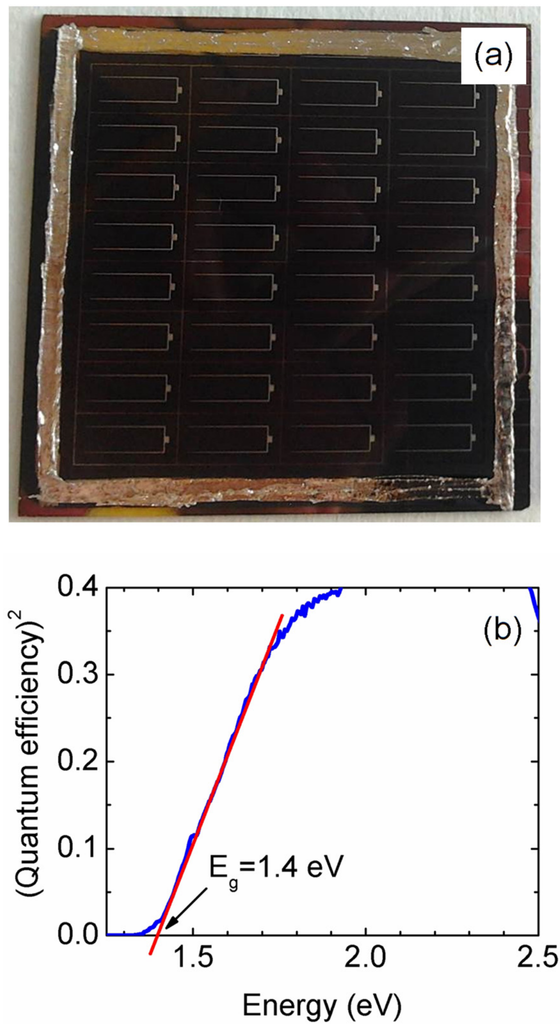

FIG. 2. (a) A completed array of CIGS/Mo PV cells (cell area 0.5 cm^2) on soda-lime glass, with the composition Cu/[Ga + In] = 78% and Ga/[Ga + In] = 68%. These exhibited an average conversion factor of 13.7%. (b) The corresponding quantum efficiency spectrum, which provides the band gap E_g of CIGS.

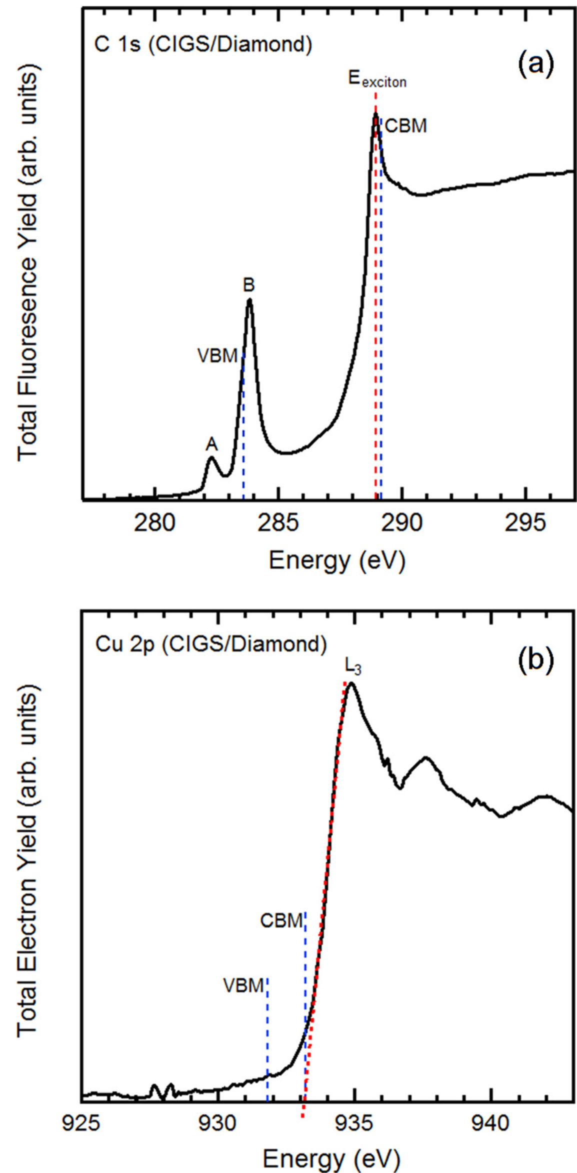

FIG. 3. XAS spectra for 7 nm CIGS deposited on a highly boron doped diamond film. (a) Bulk-sensitive C1*s* absorption spectra in the fluorescence yield detection mode. Peaks A and B are assigned to transitions into acceptor states arising from C atoms adjacent to a boron (peak A) and C atoms completely surrounded by C, but within the range of an acceptor wave function (peak B). (b) Surface-sensitive Cu2$p_{3/2}$ absorption spectra recorded in the electron yield detection mode.

is comparable to the uncertainty of the extrapolation towards the CBM (red line in Fig. 2). It would mainly affect the CBM of CIGS. XAS showed no significant differences in the spectra between the 2.3 μm and 7 nm films, and XPS gave a difference of 0.08 eV between the Cu2$p_{3/2}$ levels (Table I), which is comparable to the error bar.

Synchrotron based X-ray absorption spectroscopy studies were performed at the Advanced Light Source (ALS) at Lawrence Berkeley National Laboratory. Spectra of the CIGS/Diamond heterojunction were acquired at BL 8.0.1 to determine the unoccupied states in CIGS and diamond by probing the Cu2*p* and C1*s* edges with an energy resolution of 0.2 eV and 0.1 eV, respectively. Cu2*p* XAS spectra were recorded in the total electron yield mode by measuring the photocurrent, with a probing depth of 5–10 nm, while C1*s* spectra were recorded in the total fluorescence yield detection mode using a channel plate detector plus an Al filter, with a probing depth of *ca.* 100 nm. The photon energy was calibrated using CuO (2$p_{1/2}$ peak of CuO at 931.3 eV for Cu2*p*, compare Ref. 19) and graphite (π*-peak of graphite at 285.35 eV for C1*s*, from Ref. 20).

Hard X-ray photoemission (HXPS, HAXPES) measurements ($h\nu = 5.0$ keV) were performed at BL 9.3.1 (ALS) using a hemispherical analyzer (Scienta SES 2002), with a total resolution of 0.6 eV on the following three samples: (i) CIGS/Diamond heterojunction sample, (ii) CIGS/Mo reference sample, and (iii) H-terminated boron-doped diamond reference sample. HXPS provides information on the occupied states by probing the core levels and the valence band with respect to the Fermi level (E_F).[21] The binding energy scales were calibrated by measuring the Fermi edge of a Au reference sample. The inelastic mean free paths (IMFPs) for CIGS and diamond have been calculated for using the TPP formula[22] to be *ca.* 8 nm and 6 nm, respectively. These numbers can be compared to the much lower values of *ca.* 3 nm and 2 nm,

[This article is copyrighted as indicated in the article. Reuse of AIP content is subject to the terms at: http://scitation.aip.org/termsconditions. Downloaded to] IP: 72.33.42.248 On: Wed, 08 Oct 2014 16:28:06

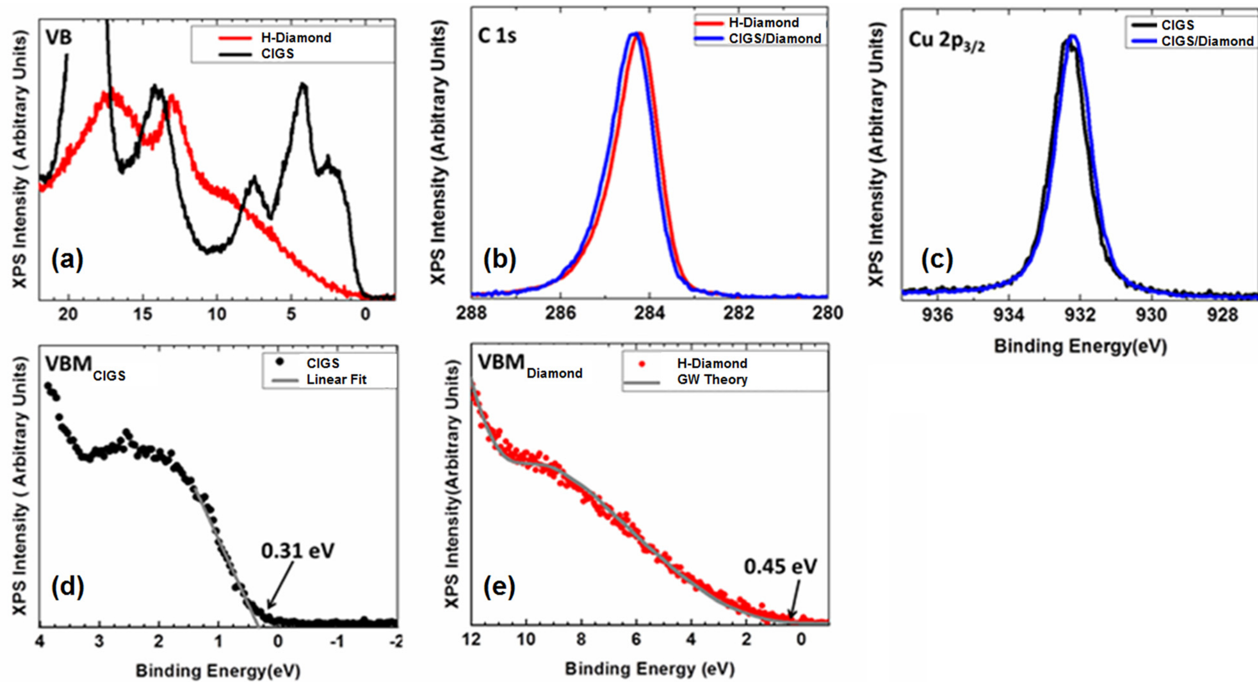

FIG. 4. XPS spectra of the CIGS/Diamond heterojunction (blue), together with bulk CIGS (black) and H-terminated diamond (red) reference samples. (a) Valence bands of reference samples. (b) C 1*s* (red: H-terminated diamond, blue: CIGS/diamond). (c) Cu $2p_{3/2}$ (black: CIGS, blue: CIGS/Diamond). (d) Valence band maximum of the bulk CIGS reference sample with linear extrapolation (gray). (e) Valence band maximum of the H-terminated diamond reference sample matched to the spectral function from a GW calculation (gray). All energies have been referenced to the Fermi level E_F via an Au sample.

again, respectively, for conventional XPS with $h\nu = 1.5$ keV. Thus, HXPS with excitation energy of $h\nu = 5$ keV permitted penetrating the 7 nm CIGS overlayer and probing the valence band offset at the CIGS/Diamond interface. This information depth is comparable to that with total electron yield detection in XAS. We have also measured the energy levels of H-terminated diamond as a reference, including its work function. The latter was obtained from the low energy cutoff of the photoelectron spectrum using a −10 V sample bias. The resulting work function of 4.97 eV is smaller than the band gap of 5.47 eV (Ref. 23) which is consistent with the negative electron affinity of H-terminated diamond.[24,25]

III. RESULTS FROM XAS

X-ray absorption spectroscopy provides information about the unoccupied states, i.e., the conduction bands of diamond and CIGS. These complement the HXPS results for the occupied states. Figure 3(a) presents the C K-edge absorption spectrum of diamond in the CIGS/Diamond sample, which reflects the onset of the C1*s* → 2*p* transitions. The excitonic peak ($E_{exciton}$) at 289.0–289.1 eV (Refs. 15, 26, 27) is shifted down from the CBM by the binding energy of the C1*s* core exciton in diamond, which is 0.19 eV.[26] That places the conduction band minimum of diamond ($CBM_{diamond}$) at 289.2–289.3 eV. Additional features in Fig. 3(a), labeled A and B (at 282.31 eV and 283.85 eV), originate from unoccupied states in the band gap that arise as a result of boron doping. They represent transitions from the C1*s* core level to the B acceptor level, which lies 0.37 eV above the VBM of diamond.[28] The upper peak matches the position of the B

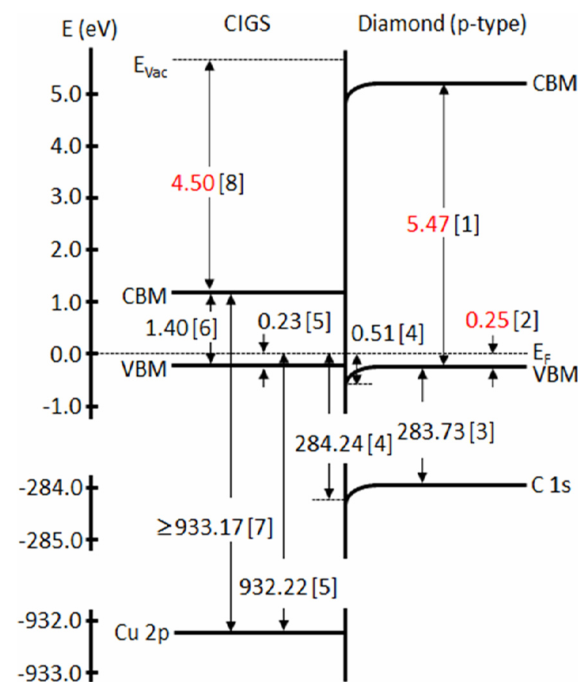

FIG. 5. Energy band diagram representing the interface between CIGS and p-doped diamond. It lists the data obtained from our HXPS, XAS, and quantum efficiency measurements, together with literature values for bulk semiconductor properties (in red). The construction of this diagram from the energy differences (1)–(8) is explained in the text. It proceeds from right to left, starting with the energy levels of bulk diamond (1)–(3) and proceeding through the interface (4) to the CIGS levels (5) –(8). All energies are referenced to the Fermi level, which remains constant throughout the interface in thermal equilibrium.

[This article is copyrighted as indicated in the article. Reuse of AIP content is subject to the terms at: http://scitation.aip.org/termsconditions. Downloaded to] IP: 72.33.42.248 On: Wed, 08 Oct 2014 16:28:06

acceptor level quite well. The lower energy peak has been assigned to transitions from C atoms adjacent to a B dopant.[15,29,30] Their C1*s* level is shifted to lower binding energy by electron transfer from the more electropositive B. The intensity ratio between peaks A and B can be rationalized by comparing the number of C atoms inside the Bohr radius of the acceptor wave function (the final state of the optical transition) with the number of C atoms adjacent to a B impurity. Additional contributions might come from interstitial B sites at high doping. These have been discussed in the literature, but have not been observed in core level spectroscopy (see Ref. 31 and references therein).

Figure 3(b) presents the Cu L_3-edge absorption spectrum of the CIGS overlayer on diamond. It is used to obtain the conduction band minimum of CIGS via linear extrapolation of the L_3 edge, following previous work.[9–11] For our CIGS film, the CBM is reached at 933.17 eV. To obtain the position of the CBM relative to the Fermi level (CBM–E_F), we subtract the Cu2$p_{3/2}$ core level binding energy obtained by HXPS. By subtracting the optical band gap from (CBM–E_F), one obtains the position of the VBM relative to E_F (VBM–E_F). The details of this procedure, together with the influence of the electron-hole interaction, are discussed with Figure 5 (Step 7).

IV. RESULTS FROM HXPS

HXPS offers a direct route to determine the valence band discontinuity or band offset at the CIGS/Diamond heterojunction, through the measurement of core level binding energies and valence-band maxima in the heterojunction and the two pure reference materials in each layer, originally developed with excitation in the conventional XPS energy regime of 1.5 keV that is less depth penetrating.[32] This method assumes a constant position of the VBM relative to a given core level in both the heterojunction and the reference materials. More specifically, the valence band maxima relative to E_F of the H-terminated diamond, and CIGS reference samples have been determined by HXPS, see Fig. 4 and Table I. In addition, core-levels representative of elements belonging exclusively to CIGS-Cu2$p_{3/2}$ and diamond-C1s have been measured with respect to E_F for the reference CIGS and H-terminated diamond samples and for the CIGS/Diamond heterojunction sample (Figs. 4(b) and 4(c)).

Once the valence band maxima of the two reference samples CIGS and H-terminated diamond (Figs. 4(d) and 4(e)), respectively, and the core-levels of the reference samples and of the heterojunction have been measured (Table I), Eq. (2) provides a direct path for the determination of the VBO in the CIGS/Diamond sample[32]

$$\Delta E_{VBO(CIGS/Diamond)} = [(E_{Cu2p3/2} - E_{VBM})_{CIGS} - (E_{C1s} - E_{VBM})_{Diamond}] - (E_{Cu2p3/2} - E_{C1s})_{CIGS/Diamond}. \quad (2)$$

$\Delta E_{VBO(CIGS/Diamond)}$ is the valence band offset of the H-terminated diamond relative to the top CIGS layer.

The valence band offset at the CIGS/Diamond heterojunction is an important parameter to characterize the energy levels of the proposed three-layer structure as discussed above. It is worthwhile to consider the terms of Eq. (2) and how accurately they can be measured. The core-levels can be accurately determined by fitting them with the Voigt function to obtain the peak positions, after subtracting the much-used Shirley background (Table I). More challenging is the accurate determination of the VBM. In the past decades, a few methods have been proposed. For example, Kraut *et al.* proposed to fit the XPS spectrum in the vicinity of the valence-band edge and determining E_{VBM} using a theoretical model, where the photoemission spectrum is assumed to be proportional to a broadened valence-band density of states (VB DOS) obtained from band structure calculations.[33] On the other hand, Chambers *et al.*[34] observed that the method of Grant *et al.* in Ref. 33 results in significant inaccuracies for VBM of complex oxide materials. They proposed fitting both the onset of the experimental spectrum near the valence band edge and the background noise (dark counts) to straight lines and then determining E_{VBM} from the intersection of these two lines. While this method is very simple to use and does not require the calculation of a theoretical VB DOS, its validity depends on the assumption of a linear VB DOS in the vicinity of E_{VBM}.

The method of Chambers *et al.* has been used to determine the VBM of the bulk CIGS reference ($VBM_{CIGS} = 0.31 \pm 0.1$ eV), Fig. 4(d).[34] However, neither this method nor that of Kraus *et al.* was able to provide an accurate VBM value of the H-terminated diamond, which has a decidedly non-linear variation near maximum and an electronic structure whose band structure is not adequately described by simple local-density calculations. We have thus gone beyond this model to determine the valence band maximum of H-terminated diamond using the *ab-initio* GW-method[35] based on quantum-mechanical many-body perturbation theory as implemented in the BerkeleyGW package,[36] which has been shown to provide a highly accurate description of the diamond band structure and bandgap.[35,37] A detailed discussion of the VBM determination in a system such as diamond with mixed valence band states (C2*s* and C2*p*) and showing a strong dependence of their orbital cross-section as a function of the excitation energy is reported elsewhere.[37] The fit of the GW-method curve to the measured H-terminated diamond valence band edge gives a VBM $= 0.45 \pm 0.2$ eV, as shown in Fig. 4(e).

The VBO at the interface between diamond (bottom layer) and CIGS (top layer) is determined from the HXPS data in Table I via Eq. (2): $VBO_{CIGS/Diamond} = (VBM_{CIGS} - VBM_{diamond}) = 0.27 \pm 0.2$ eV. The VBM of CIGS lies somewhat higher than the VBM of diamond at the interface and thus creates a shallow barrier for electron donation from diamond. The VBMs at the interface can be determined from those of the reference samples by taking the difference of the core level energies into account, using the following equations. These reflect the fact that the energy difference between the VBM and a core level is not affected by band bending or surface termination

[This article is copyrighted as indicated in the article. Reuse of AIP content is subject to the terms at: http://scitation.aip.org/termsconditions. Downloaded to] IP: 72.33.42.248 On: Wed, 08 Oct 2014 16:28:06

$$\mathrm{VBM}^{\mathrm{Interface}}_{\mathrm{Diamond}} = (\mathrm{C}1s)_{\mathrm{CIGS/Diamond}} - (\mathrm{C}1s - \mathrm{VBM})_{\mathrm{Diamond}}$$
$$\mathrm{VBM}^{\mathrm{Interface}}_{\mathrm{CIGS}} = (\mathrm{Cu}2p_{3/2})_{\mathrm{CIGS/Diamond}} - (\mathrm{Cu}2p_{3/2} - \mathrm{VBM})_{\mathrm{CIGS}}. \quad (3)$$

The upper equation will also be used in Sec. V to increase the accuracy of the VBM of diamond by using an accurate literature value for $(\mathrm{C}1s - \mathrm{VBM})_{\mathrm{Diamond}}$.

V. COMBINATION OF XAS, HXPS, AND OTHER AVAILABLE DATA

In order to obtain the most complete and accurate results possible, we have combined our own data from XAS, HXPS, and quantum efficiency measurements with literature values and our computed GW values for bulk energy levels of diamond, such as the band gap E_g, $(E_F - \mathrm{VBM})$, and $(\mathrm{VBM} - \mathrm{C}1s)$. The resulting band diagram in Fig. 5 is constructed from the right side (bulk diamond) to the left (bulk CIGS) in 8 steps, which are explained in detail below the figure. We begin with two accurately known properties of bulk diamond, the band gap of 5.47 eV and the position of the VBM relative to the Fermi level E_F (which can be calculated accurately from bulk electrical properties versus temperature and B doping). Since E_F remains constant throughout the interface in thermal equilibrium, it becomes the natural reference level. Relative to E_F, the band edges and core levels exhibit band bending near the interface due to the electrostatic potential in the space charge region. To track the movement of the broad VBM through the band bending region, we use the sharp C1*s* core level, as quantified in Eq. (3). This can be done, since the energy difference (VBM–C1*s*) is a basic electronic structure property of bulk diamond that is not affected by band bending or surface termination. The most accurate determination of (VBM–C1*s*) from the literature is combined with the energy of the C1*s* level at the interface, as measured by HXPS. Next, we move further to the left in Fig. 5 across the interface into the CIGS film. HXPS and XAS probe both the bulk and the two surfaces of the thin CIGS film, such that the resulting energies represent an average across the film. The VBM in CIGS is well-pronounced in HXPS and can be obtained relative to E_F from the data in Fig. 4(a). Adding the band gap obtained from the quantum efficiency spectrum in Fig. 2 gives the CBM in CIGS. The result for the CBM of CIGS can be cross-checked by using the onset of the conduction band transitions in the $\mathrm{Cu}2p_{3/2}$ XAS spectrum of Fig. 3 and subtracting the HXPS binding energy of the $\mathrm{Cu}2p_{3/2}$ core level in Fig. 4(c). The CBM value is extracted from the onset of the $\mathrm{Cu}2p_{3/2}$ XAS by linear extrapolation, using a previously established method.[9–11] Finally, one can take the electron affinity of CIGS from the literature[36] to assign a vacuum level E_{vac} to the CIGS film.

The energy level diagram in Fig. 5 originates from a variety of measurements in order to obtain the highest possible accuracy and to estimate the error bars by cross-checks between several methods. Energies are given with two decimals (where available) in order to avoid rounding errors when adding or subtracting multiple energies. The following sequence of steps establishes the diagram:

(1) The band gap of diamond (5.47 eV) is obtained from Clark *et al.*,[23] see also Bandis and Pate.[39] Notice that there are two opposing effects shifting the onset of the optical absorption. The valence exciton binding energy of 70–80 meV lowers the threshold, and the excitation of a phonon required by the indirect band gap increases the threshold by 83 meV and 160 meV (for TA and TO phonons, respectively). At room temperature, one has also phonon absorption, which lowers the threshold.
(2) The bulk Fermi level in highly doped diamond lies slightly below the B acceptor level, which is 0.37 eV above the VBM.[28] For our doping level of about $10^{20}\,\mathrm{cm}^{-3}$, the calculation by Diederich *et al.*[25] gives $(E_F - \mathrm{VBM}) = 0.25$ eV.
(3) The energy difference (VBM–C1*s*) is a key quantity characteristic of bulk diamond. It is independent of the surface termination, Fermi level pinning, and band bending, since it is determined by the C-C interaction. Here, we discuss three methods to obtain this quantity. Their comparison allows an estimate of the accuracy.

The most accurate method starts with the sharp negative electron affinity peak (0.5 eV FWHM) which is observed in the secondary electron spectrum of H-terminated diamond.[24,25] It represents electrons piled up at the CBM. The energy of this peak was combined with the C1s level measured for the same sample by Morar *et al.*[26] to give (CBM–C1s) = 289.20 eV. Subtracting the band gap of 5.47 eV (Ref. 23) from step (1) gives (VBM–C1*s*) = (CBM–C1*s*) $- E_g$ = 283.73 eV.

A second method uses the difference between the onset of the valence band and the C1s peak obtained from HXPS. This method suffers from the low intensity and slow onset of the valence band maximum (several eV wide), particularly at high photon energies (Fig. 4(e)). The combination of HXPS with GW calculations in Fig. 4 minimizes these uncertainties and gives (VBM–C1*s*) = 284.19 eV–0.45 eV = 283.74 eV for H-terminated diamond (Table I). An earlier XPS result by Shi *et al.*[40] gave (VBM–C1*s*) = 284.90 eV − 1.32 eV = 283.58 eV, but this work employed a lower excitation energy of ∼1.5 keV and a less accurate method to obtain the VBM (linear extrapolation of the leading edge spectra to the baseline).

A third method starts with the C1*s* exciton peak observed in XAS at 289.0 eV by Morar *et al.*[26] This value is consistent with our result of 289.0 eV and the recent value of 289.1 eV obtained by Zegkinoglou *et al.*[15] within the error bar of ±0.1 eV for the absolute energy calibration in XAS. After adding the exciton binding energy of 0.19 eV (Ref. 26) to obtain the CBM and subtracting the band gap of 5.47 eV (Ref. 23), we obtain (VBM–C1*s*) = 283.7 eV ± 0.1 eV.

Overall, the values obtained for (VBM–C1*s*) in diamond from the three methods range from 283.58 eV to 283.8 eV, with 283.73 ± 0.1 eV as the most accurate value.

(4) The energy difference $(E_F - \mathrm{C}1s) = 284.24$ eV at the CIGS/Diamond interface is obtained from our HXPS results in Fig. 4 and Table I. Subtracting the best value of (VBM–C1*s*) = 283.73 eV obtained in step (3) gives (E_F–VBM) = 0.51 eV at the interface. Comparing this with the bulk value of (E_F–VBM) = 0.25 eV from step

[This article is copyrighted as indicated in the article. Reuse of AIP content is subject to the terms at: http://scitation.aip.org/termsconditions. Downloaded to] IP: 72.33.42.248 On: Wed, 08 Oct 2014 16:28:06

(2) gives a band bending of 0.26 eV. Notice that this value is a lower limit, obtained with the assumption that the HXPS escape depth is small compared to the width of the band bending region.

(5) The energy differences (E_F–Cu2$p_{3/2}$) = 932.22 eV and (E_F–VBM) = 0.23 eV for CIGS/Diamond are obtained from our HXPS results in Fig. 4 and Table I. These are averaged over the thickness of the CIGS film by HXPS. Comparing the values of (E_F–VBM) at both sides of the CIGS/Diamond interface from steps (4) and (5), one obtains a valence band offset ($VBM_{CIGS} - VBM_{diamond}$) = (0.51 eV − 0.23 eV) = 0.28 eV, with the VBM of CIGS lying higher. The offset to the bulk valence band of diamond is (0.25 eV − 0.23 eV) = 0.02 eV using (2).

(6) The CIGS band gap E_g = 1.4 eV is obtained from the quantum efficiency measurement in Fig. 2(a). By adding it to the VBM from step (5) (0.23 eV below E_F for CIGS/Diamond), one obtains the CBM in CIGS/Diamond at 1.17 eV above E_F.

(7) The CBM in CIGS/Diamond can be obtained independently by combining HXPS with XAS at the Cu2$p_{3/2}$ edge. This yields a lower limit of the energy difference (CBM–Cu2$p_{3/2}$) ≥ 933.17 eV for CIGS/Diamond is obtained from our XAS in Fig. 3, using linear extrapolation towards the onset and assuming that the electron-hole interaction is negligible. Compare similar results and extrapolation methods in Bär *et al.*,[9] Johnson *et al.*,[10] and Bär *et al.*[11] Combining this result with (E_F–Cu2$p_{3/2}$) = 932.22 eV for CIGS/Diamond from step (5) gives (CBM–E_F) ≥ 0.95 eV. With E_g from step (7), we obtain (E_F–VBM) ≤ 0.45 eV in CIGS. This value is less accurate that the result of 0.23 eV obtained directly from HXPS in step (3). It involves several measurements (XAS, HXPS, and quantum efficiency), and the XAS result for the CBM of CIGS may be affected by electron-hole-interaction. In that case, the actual CBM would lie higher above E_F, and the VBM would be closer to E_F. An electron-hole interaction of 0.22 eV would bring the two measurements into agreement.

(8) The vacuum level of CIGS is obtained by adding the electron affinity of CIGS (4.5 eV) from Hossain *et al.*[38] to the CBM from step (6).

VI. CONCLUSIONS

In summary, we have determined the energy level diagram for a CIGS absorber combined with a diamond donor using a variety of techniques that are cross-checked against each other to obtain the most reliable results. The valence band maximum of CIGS lies very close to that of bulk diamond (within our error bar of ±0.1 eV), as required for refilling the photogenerated holes in the CIGS absorber via the diamond film. That provides a good starting point for optimizing the band offset. However, the band bending at the interface still creates a barrier of ≥0.3 eV at the interface, which would need to be overcome by sufficiently high doping. This seems possible, as boron-doped diamond can actually be doped high enough to become metallic and even superconducting.[41] One could also push the valence band maximum of the absorber film a few tens of an eV lower to ensure that the photo-generated holes are refilled quickly enough to prevent recombination with photogenerated electrons. For example, substitution of Se with S lowers the VBM in CIGS. Overall, our findings are of generic interest for new solar cell designs involving transparent electron donor and acceptor materials.

ACKNOWLEDGMENTS

This work was supported by the Department of Energy, Basic Energy Sciences, under Contract Nos. DE-SC0006931, DE-AC02-05CH11231 (ALS), and DE-FG02-01ER45917 (end station). The authors thank Dr. Lyuba Belova and Dr. Anastasia Riazanova at Royal Institute of Technology for their timely help with high-resolution electron microscopy studies on the morphology of the CIGS samples. G.C, S.N., C.S.C., and C.F. also acknowledge the support of the Department of Energy, Basic Energy Sciences, under Contract DE-AC02-05CH11231, via the Lawrence Berkeley National Laboratory Materials Sciences Division. R.J.H. and L.Z. acknowledge the National Science Foundation DMR-1207281 (diamond sample preparation). Theoretical studies were supported by the SciDAC Program on Excited State Phenomena in Energy Materials funded by the U. S. Department of Energy, Basic Energy Sciences and Advanced Scientific Computing Research, under Contract No. DE-AC02-05CH11231 at the Lawrence Berkeley National Laboratory (GW quasiparticle computations and algorithm and code development), and by the National Science Foundation under grant DMR10-1006184 (basic theory and analysis). C.S.F. is also grateful for support from the APTCOM Project of the Triangle de Physique, Paris.

[1] A chart of solar cell efficiencies is given by NREL at http://www.nrel.gov/ncpv/images/efficiency_chart.jpg.
[2] F. J. Himpsel, P. L. Cook, G. de la Torre, J. M. Garcia-Lastra, R. Gonzalez-Moreno, J.-H. Guo, R. J. Hamers, C. X. Kronawitter, P. S. Johnson, J. E. Ortega, D. Pickup, M.-E. Ragoussi, C. Rogero, A. Rubio, R. E. Ruther, L. Vayssieres, W. Yang, and I. Zegkinoglou, J. Electron Spectrosc. Relat. Phenom. **190**, 2 (2013).
[3] P. Jackson, D. Hariskos, E. Lotter, S. Paetel, R. Wuerz, R. Menner, W. Wischmann, and M. Powalla, Prog. Photovoltaics **19**, 894 (2011).
[4] I. Repins, M. A. Contreras, B. Egaas, C. DeHart, J. Scharf, C. L. Perkins, B. To, and R. Noufi, Prog. Photovoltaics **16**, 235 (2008).
[5] M. Kapilashrami, C. X. Kronawitter, T. Törndahl, J. Lindahl, A. Hultqvist, W.-C. Wang, C.-L. Chang, S. S. Mao, and J.-H. Guo, Phys. Chem. Chem. Phys. **14**, 10154 (2012).
[6] K. Orgassa, H. W. Schock, and J. H. Werner, Thin Solid Films **387**, 431 (2003).
[7] L. Weinhardt, O. Fuchs, A. Peter, E. Umbach, C. Heske, J. Reichardt, M. Bär, I. Lauermann, I. Kötschau, A. Grimm, S. Sokoll, M. Ch. Lux-Steiner, T. P. Niesen, S. Visbeck, and F. Karg, J. Chem. Phys. **124**, 074705 (2006).
[8] M. Bär, S. Nishiwaki, L. Weinhardt, S. Pookpanratana, W. N. Shafarman, and C. Heske, Appl. Phys. Lett. **93**, 042110 (2008).
[9] M. Bär, L. Weinhardt, S. Pookpanratana, C. Heske, S. Nishiwaki, W. Shafarman, O. Fuchs, M. Blum, W. Yang, and J. D. Denlinger, Appl. Phys. Lett. **93**, 244103 (2008).
[10] B. Johnson, J. Klaer, S. Merdes, M. Gorgoi, B. Höpfner, A. Vollmer, and I. Lauermann, J. Electron. Spectrosc. Relat. Phenom. **190**, 42 (2013).
[11] M. Bär, S. Pookpanratana, L. Weinhardt, R. G. Wilks, B. A. Schubert, B. Marsen, T. Unold, M. Blum, S. Krause, Y. Zhang, A. Ranasinghe, K. Ramanathan, I. Repins, M. A. Contreras, S. Nishiwaki, X. Liu, N. R. Paudel, O. Fuchs, T. P. Niesen, W. Yang, F. Karg, A. D. Compaan, W. N. Shafarman, R. Noufi, H.-W. Schock, and C. Heske, J. Electron. Spectrosc. Relat. Phenom. **190**, 47 (2013).

[This article is copyrighted as indicated in the article. Reuse of AIP content is subject to the terms at: http://scitation.aip.org/termsconditions. Downloaded to] IP: 72.33.42.248 On: Wed, 08 Oct 2014 16:28:06

[12] A. Kraft, Int. J. Electrochem. Sci. **2**, 355 (2007).
[13] D. M. Gruen, A. R. Krauss, C. D. Zuiker, R. Csencsits, L. J. Terminello, J. A. Carlisle, I. Jimenez, D. G. J. Sutherland, D. K. Shuh, W. Tong, and F. J. Himpsel, Appl. Phys. Lett. **68**, 1640 (1996).
[14] W. S. Yeap, X. Liu, D. Bevk, L. Lutsen, M. Fahlman, W. Maes, and K. Haenen, ACS Appl. Mater. Interfaces **6**, 10322 (2014).
[15] I. Zegkinoglou, P. L. Cook, P. S. Johnson, W. Yang, J.-H. Guo, D. Pickup, R. Gonzalez-Moreno, C. Rogero, R. E. Ruther, M. L. Rigsby, J. E. Ortega, R. J. Hamers, and F. J. Himpsel, J. Phys. Chem. C **116**, 13877 (2012).
[16] T. Strother, T. Knickerbocker, J. N. Russell, Jr., J. E. Butler, L. M. Smith, and R. J. Hamers, Langmuir **18**, 968 (2002).
[17] J. Lindahl, U. Zimmermann, P. Szaniawski, T. Torndahl, A. Hultqvist, P. Salom, C. Platzer-Bjorkman, and M. Edoff, IEEE J. Photovoltaics **3**(3), 1100 (2013).
[18] M. I. Alonso, M. Garriga, C. A. Durante Rincon, E. Hernández, and M. Leon, Appl. Phys. A **74**, 659 (2002).
[19] P. L. Cook, W. Yang, X. Liu, J. M. García-Lastra, A. Rubio, and F. J. Himpsel, J. Chem. Phys. **134**, 204707 (2011).
[20] E. J. Mele and J. J. Ritsko, Phys. Rev. Lett. **43**, 68 (1979).
[21] E. A. Kraut, R. W. Grant, J. R. Waldrop, and S. P. Kowalczyk, Phys. Rev. B **28**, 1965 (1983).
[22] S. Tanuma, C. J. Powell, and D. R. Penn, Surf. Int. Anal. **20**, 77 (1993).
[23] C. D. Clark, P. J. Dean, and P. V. Harris, Proc. R. Soc. London, Ser. A **277**, 312 (1964).
[24] F. J. Himpsel, J. A. Knapp, J. A. Van Vechten, and D. E. Eastman, Phys. Rev. B **20**, 624 (1979).
[25] L. Diederich, O. M. Kuttel, P. Aebi, and L. Schlapbach, Surf. Sci. **418**, 219 (1998).
[26] J. F. Morar, F. J. Himpsel, G. Hollinger, G. Hughes, and J. L. Jordan, Phys. Rev. Lett. **54**, 1960 (1985).
[27] P. E. Batson and J. Bruley, Phys. Rev. Lett. **67**, 350 (1991).
[28] A. T. Collins and A. W. S. J. Williams, Physica C **13**, 1789 (1971); B. Massarani and J. C. Bourgoin, Phys. Rev. B **17**, 1758 (1978); J. C. Bourgoin, J. Krynicki, and B. Blanchar, Phys. Status Solidi A **52**, 293 (1979).
[29] J. Nakamura, N. Yamada, K. Kuroki, T. Oguchi, K. Okada, Y. Takano, M. Nagao, I. Sakaguchi, T. Takenouchi, H. Kawarada, R. C. C. Perera, and D. L. Ederer, J. Phys. Soc. Jpn. **77**, 054711 (2008).
[30] P.-A. Glans, T. Learmonth, K. E. Smith, S. Ferro, A. De Battisti, M. Mattesini, R. Ahuja, and J.-H. Guo, Appl. Phys. Lett. **102**, 162103 (2013).
[31] Y. Kato, F. Matsui, T. Shimizu, H. Daimon, T. Matsushita, and F. Z. Guo, Appl. Phys. Lett. **91**, 251914 (2007).
[32] S. A. Chambers, Y. Liang, Z. Yu, R. Droopad, J. Ramdani, and K. Eisenbeiseret, Appl. Phys. Lett. **77**, 1662 (2000).
[33] R. W. Grant, J. R. Waldrop, and E. A. Kraut, J. Vac. Sci. Tec. **15**, 1451 (1978); E. A. Kraut, R. W. Grant, J. R. Waldrop, and S. P. Eowalczyk, Phys. Rev. Lett. **44**, 1620 (1980).
[34] S. A. Chambers, T. Droubay, T. C. Kaspar, and M. Gutowski, J. Vac. Sci. Technol. B **22**, 2205 (2004).
[35] M. S. Hybertsen and S. G. Louie, Phys. Rev. B **34**, 5390 (1986).
[36] J. Deslippe, G. Samsonidze, M. Jain, M. L. Cohen, and S. G. Louie, Comput. Phys. Commun. **183**, 1269 (2012).
[37] J. Lischner, S. Nemsak, G. Conti, G. K. Palsson, A. Hloskovsky, W. Drube, C. Fadley, and S. G. Louie, "Accurate determination of the valence band edge in hard x-ray photoemission spectra by means of GW theory" (unpublished).
[38] M. I. Hossain, P. Chelvanathan, M. Zaman, M. R. Karim, M. A. Alghoul, and N. Amin, Chalcogenide Lett. **8**(5), 315 (2011).
[39] C. Bandis and B. B. Pate, Phys. Rev. Lett. **74**, 777 (1995); Phys. Rev. B **52**, 12056 (1995).
[40] K. Shi, X. L. Liu, D. B. Li, J. Wang, H. P. Song, X. Q. Xu, H. Y. Wei, C. M. Jiao, S. Y. Yang, H. Song, Q. S. Zhu, and Z. G. Wang, Appl. Surf. Sci. **257**, 8110 (2011).
[41] K. Ishizaka, R. Eguchi, S. Tsuda, A. Chainani, T. Yokoya, T. Kiss, T. Shimojima, T. Togashi, S. Watanabe, C.-T. Chen, Y. Takano, M. Nagao, I. Sakaguchi, T. Takenouchi, H. Kawarada, and S. Shin, Phys. Rev. Lett. **100**, 166402 (2008).

[This article is copyrighted as indicated in the article. Reuse of AIP content is subject to the terms at: http://scitation.aip.org/termsconditions. Downloaded to] IP: 72.33.42.248 On: Wed, 08 Oct 2014 16:28:06